Design, Synthesis, and Pharmacological Evaluation of Pyridinic Analogues of Nimesulide as Cyclooxygenase-2 Selective Inhibitors

Fabien Julémont,*[,||,†] Xavier de Leval,[||,†] Catherine Michaux,[‡] Jean-François Renard,[†] Jean-Yves Winum,[§] Jean-Louis Montero,[§] Jacques Damas,[#] Jean-Michel Dogné,[†] and Bernard Pirotte[†]

Natural and Synthetic Drugs Research Centre, Laboratory of Medicinal Chemistry, Université de Liège, 1, Avenue de l'Hôpital, B36, B-4000 Liège, Belgium, Department of Molecular and Structural Chemistry, Université de Namur, 61, Rue de Bruxelles, B-5000 Namur, Belgium, Laboratoire de Chimie Biomoléculaire, Université Montpellier II, UMR 5032, ENSCM, 8, Rue de l'Ecole Normale, 34296 Montpellier Cedex, France, and Department of Human Physiology, Université de Liège, 1, Avenue de l'Hôpital, B23, B-4000 Liège, Belgium

Received June 30, 2004

In this study, we report the synthesis and pharmacological evaluation of original pyridinic sulfonamides related to nimesulide, a cyclooxygenase-2 (COX-2) preferential inhibitor widely used as an anti-inflammatory agent. These original pyridinic derivatives were synthesized in three steps starting from the condensation of 3-bromo-4-nitropyridine *N*-oxide with appropriately substituted phenols, thiophenols, or anilines followed by a reduction of the nitro moiety into the corresponding aminopyridine, which was finally condensed with alkane- or trifluoromethanesulfonyl chloride to obtain the corresponding sulfonamides. The pK_a determinations demonstrated that the major ionic form present in solution at physiological pH depends on the nature of the sulfonamide moiety subsituent. Indeed, alkanesulfonamides were mainly present as zwitterionic molecules while trifluoromethanesulfonamides, more acidic derivatives, were mainly present as anionic molecules. The in vitro pharmacological evaluation of the synthesized compounds against COX-1 and COX-2 was performed in a human whole blood model. Results obtained demonstrated that most of alkanesulfonamide derivatives displayed a COX-2 preferential inhibition with selectivity ratio values (IC_{50}(COX-1)/IC_{50}(COX-2)) up to 7.92 (celecoxib displaying a ratio value of 7.46 in the same test). On the other hand, trifluoromethanesulfonamide derivatives displayed weaker selectivity ratios although they exhibited IC_{50} values against COX-2 up to 0.09 μM (celecoxib IC_{50} against COX-2: 0.35 μM). Finally, *in vivo* evaluation of selected compounds showed that they exhibited anti-inflammatory properties similar to that of nimesulide when tested in a carrageenan-induced rat paw oedema model.

Introduction

Cyclooxygenase (prostaglandin endoperoxide synthase or COX) compounds catalyze the transformation of arachidonic acid into prostaglandin H_2 (PGH_2), the first step in the biosynthesis of prostanoids (prostaglandins, prostacyclin, and thromboxane), which are local mediators acting in an auto- or paracrine manner through their binding to specific receptors. Three COX isozymes are actually described: COX-1, COX-2, and COX-3. COX-1 is an ubiquitous constitutive form of the enzyme responsible for the basal levels of prostanoids involved in the regulation of several physiological processes such as the platelet aggregation or the homeostasis of the gastrointestinal tract and kidneys. The COX-2 isozyme is almost undetectable under physiologic conditions although its expression can be induced by a wide range of stimuli such as growth factors,[1,2] phorbol esters,[3] interleukin-1 (IL-1)[4−6] or lipopolysaccharide (LPS).[7−9] COX-2 expression is mainly observed during inflammatory processes and is responsible for the enhanced prostanoid biosynthesis observed under these pathological conditions. Finally, a third COX isoform, COX-3, located in the central nervous system has recently been characterized and could be the pharmacological target of acetaminophen.

Acting as nonselective COX inhibitors, classical nonsteroidal anti-inflammatory drugs (NSAIDs) have been widely used in the treatment of acute and chronic inflammation states. However, all these drugs cause untoward side effects related to COX-1 inhibition, among which gastrointestinal irritation leading to ulcers and bleeding is the most common.[10,11] On the other hand, COX-2 specific inhibitors display anti-inflammatory, antipyretic and analgesic properties in several animal and human models. These pharmacological properties are correlated to their ability to decrease the COX-2-dependent prostanoid biosynthesis. These data clearly demonstrate the implication of COX-2 in inflammation processes. Furthermore, prostanoids are also involved in other pathological conditions such as cancer progression. Indeed, because they affect mitogenesis,[12] cellular adhesion[13] and apoptosis,[14] prostaglandins appear to play a major role in the pathogenesis of several types of cancers such as head and neck,[15] breast,[16,17] lung,[18,19] colon,[20,21] pancreas,[22] and prostate[23] cancers where an important COX-2 expression has been

* To whom correspondence should be addressed. Phone: 32-4-3664381. Fax: 32-4-3664362. E-mail: f.julemont@ulg.ac.be.
|| The two first authors contributed equally.
† Laboratory of Medicinal Chemistry, Université de Liège.
‡ Université de Namur.
§ Université Montpellier II.
# Department of Human Physiology, Université de Liège.

10.1021/jm049480l CCC: $27.50
Published on Web 12/07/2004

Scheme 1[a]

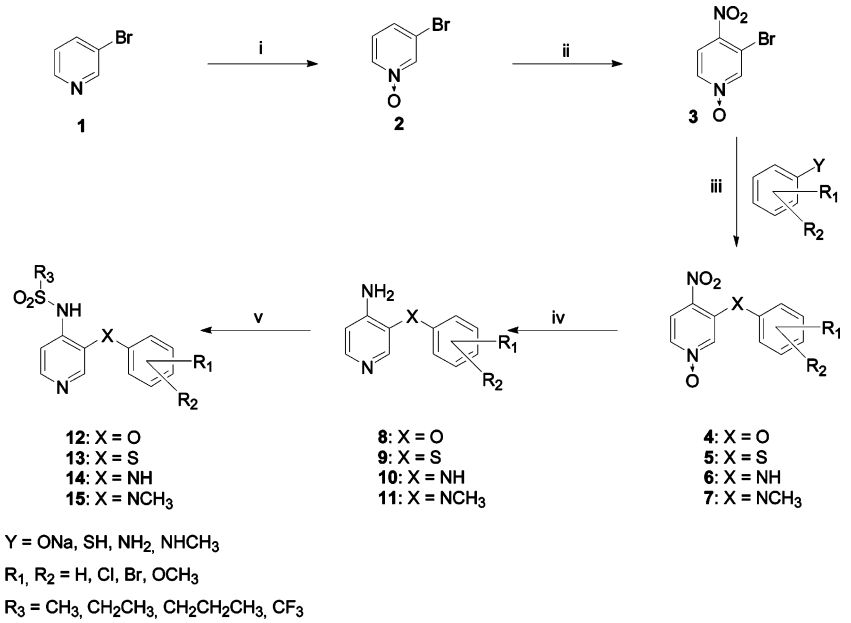

[a] Reagents: (i) H_2O_2, CH_3COOH; (ii) HNO_3, H_2SO_4; (iii) K_2CO_3; (iv) Fe, CH_3COOH/H_2O; (v) R_3SO_2Cl, K_2CO_3.

demonstrated by immunohistochemistry. Furthermore, COX-2 expression has been demonstrated to contribute to angiogenesis, a critical step in tumor vascularization and subsequently development.[24] The large body of literature indicates the effectiveness of COX-2 inhibitors in the prevention of cancer progression or treatment. For example, celecoxib has been demonstrated to induce an adenoma regression in a placebo-controlled trial in familial adenomatous polyposis patients.[25] The mechanism by which COX inhibitors display anticancer properties is also related to their ability to inhibit the prostanoid biosynthesis, although other non-prostanoid-dependent mechanisms, such as the inhibitory properties of celecoxib against human carbonic anhydrase IX (hCAIX),[26] a carbonic anhydrase isozyme overexpressed in several cancer types, have also been demonstrated. In conclusion, the evidence of therapeutic benefit deriving from selective COX-2 inhibition in pathological conditions such as inflammatory states or cancer progression has led to the development of a large number of COX-2 preferential inhibitors.

At the present time, two major classes of compounds are presented as COX-2 selective inhibitors. The first one is the methanesulfonamide class whose main investigated compounds are nimesulide, NS-398, and flosulide. The second is the "coxib" family, which is considered as the most promising class. Major compounds of this family are celecoxib, rofecoxib, and valdecoxib[27] (Figure 1). In a previous study,[28] we have demonstrated that pyridinic analogues of nimesulide are potential COX inhibitors. The aim of our present work is the development of a NSAID displaying a COX-2 preferential inhibitory profile in order to avoid the classical side effects related to COX-1 inhibition. Herein, we report the modulation of our lead compounds achieved in order to obtain COX-2 selective inhibitors. The influences of the susbtituent on the phenyl ring, the nature of the intercycle linkage, and the sulfonamide moiety have been investigated. The synthesized compounds were pharmacologically evaluated in a whole blood assay for COX-1 and COX-2 inhibition *in vitro*. Secondly, selected compounds were also evaluated as anti-inflammatory drugs *in vivo*. Finally, to understand differences in COX inhibition for closely related compounds, crystallographic and docking studies were also performed.

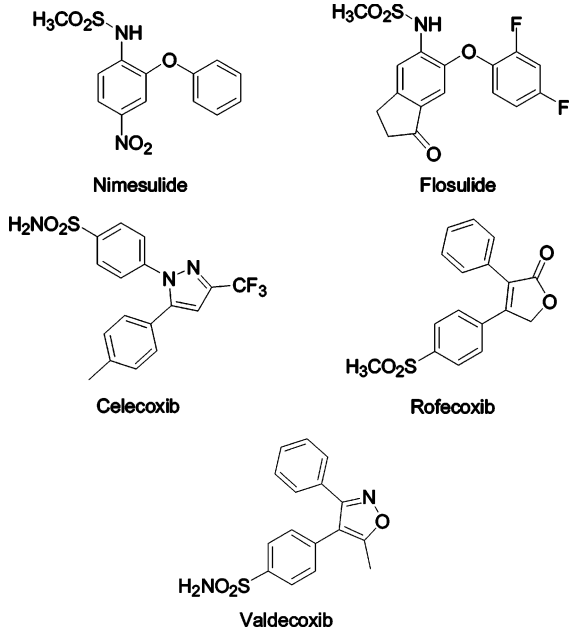

Figure 1. Chemical structures of COX-2 inhibitors.

Chemistry

The synthesis of our compounds begins with the preparation of 3-bromo-4-nitropyridine *N*-oxide (compound **3**), the common intermediate derivative (Scheme 1). This synthesis was achieved in two steps, starting with the oxidation of 3-bromopyridine **1** by hydrogen peroxide in the presence of acetic acid. This oxidation was followed by a nitration at the 4-position of the pyridine *N*-oxide **2** in a mixture of nitric acid and sulfuric acid at 90 °C for 5 h in order to obtain **3**, a

Scheme 2[a]

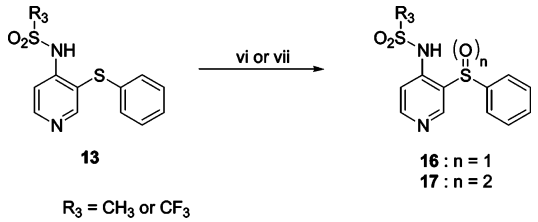

[a] Reagents: (vi) *m*-CPBA, CH_2Cl_2; (vii) H_2O_2, CH_3COOH.

yellow solid. Following this step, the bromine atom was substituted with appropriately substituted sodium phenolate such as 4-chlorophenolate under reflux to achieve compounds **4a**−**h**. Compound **5**, the thio analogue of **4a**, was obtained by reaction of **3** and thiophenol under reflux in toluene for 12 h. Finally, the reaction of **3** and aniline or *N*-methylaniline led to compounds **6** and **7**, respectively. The nitro and the *N*-oxide functions of compounds **4a**−**h** and **5**−**7** were then reduced in one step with iron in an acetic acid and water mixture to afford the corresponding aminopyridines as oily compounds (compounds **8a**−**h** and **9**−**11**). These aminopyridines were used without further purification. The sulfonamides were obtained by reaction of the aminopyridines with the suitable sulfonyl chloride (methyl, ethyl, propyl, or trifluoromethanesulfonyl chloride). As presented in Scheme 2, compounds **16b** and **17b** were synthesized by oxidation of **13b** at room temperature, using *m*-chloroperoxybenzoic acid (*m*-CPBA) in dichloromethane or hydrogen peroxide in acetic acid, respectively. A summary of the synthesized compounds is presented in Table 1.

pK_a Determination

The determination of the ionic state of the synthesized compounds at the physiological pH of 7.4 was deduced from the pK_a values. The pK_a values were obtained by UV spectrophometry according to our previously described method,[28] and the results obtained are presented in Table 2. To determine the influence of the phenyl ring substitution, the pK_a values obtained for compounds **12a**,**c**−**e**,**g** were compared. For these compounds, two pK_a values were obtained. The lower pK_a values were inferior to **4** and were not determined with more precision. According to our first report[28] and to the chemical structure of the investigated compounds, these values were assigned to the pK_a value of the sulfonamide/sulfonamidate equilibrium while the higher ones were assigned to the pyridinium/pyridine equilibrium (see Figure 2). These data permitted us to conclude that the introduction of a substituent like a halogen atom or a methoxy group led to compounds mainly present under their zwitterionic forms at physiological pH (pyridinium compounds substituted by a sulfonamidate group), as does the parent compound **12a**. The introduction of a halogen atom on the phenyl ring does not influence the major ionic form present in solution at physiological pH. Inversely, comparison of the pK_a values obtained with compounds **12a**,**i**,**d**,**m** led to the conclusion that the replacement of the methanesulfonamide group by a trifluoromethanesulfonamide group enhances the acidic character of these compounds. Therefore, compounds bearing a trifluoromethanesulfonamide moiety are mainly present at physiological

Table 1. Synthesized Compounds

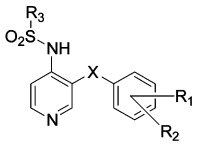

	R_1	R_2	R_3	X
12a	H	H	CH_3	O
12b	2-Cl	H	CH_3	O
12c	3-Cl	H	CH_3	O
12d	4-Cl	H	CH_3	O
12e	4-Br	H	CH_3	O
12f	4-OCH_3	H	CH_3	O
12g	2-Cl	4-Cl	CH_3	O
12h	3-Cl	5-Cl	CH_3	O
12i	H	H	CF_3	O
12k	2-Cl	H	CF_3	O
12l	3-Cl	H	CF_3	O
12m	4-Cl	H	CF_3	O
12n	4-Br	H	CF_3	O
12o	4-OCH_3	H	CF_3	O
12p	2-Cl	4-Cl	CF_3	O
12q	3-Cl	5-Cl	CF_3	O
12r	H	H	CH_2CH_3	O
12s	4-Cl	H	CH_2CH_3	O
12t	H	H	$CH_2CH_2CH_3$	O
12u	4-Cl	H	$CH_2CH_2CH_3$	O
13a	H	H	CH_3	S
13b	H	H	CF_3	S
14b	H	H	CF_3	NH
15b	H	H	CF_3	NCH_3
16b	H	H	CF_3	SO
17a	H	H	CH_3	SO_2
17b	H	H	CF_3	SO_2

Table 2. pK_a Values Determined for Selected Compounds

compds	pK_{a1}	pK_{a2}
12a	2.98 ± 0.11	8.13 ± 0.03
12c	<4	7.74 ± 0.19
12d	<4	7.97 ± 0.08
12e	<4	7.86 ± 0.03
12g	<4	7.81 ± 0.05
12i	<1	6.81 ± 0.21
12m	<1	6.71 ± 0.34
12s	<4	7.98 ± 0.05
13b	<1	6.54 ± 0.26
16b	<1	5.69 ± 0.17
17b	<1	5.30 ± 0.07

pH as anionic molecules (pyridine derivatives substituted with a sulfonamidate function). On the other hand, the replacement of the methanesulfonamide moiety by an ethanesulfonamide resulted in a minor change of the pK_a value (comparison between the pK_a values obtained for compounds **12d** and **12s**). Like the methanesulfonamide compounds, the ethane- and propanesulfonamide derivatives are expected to be mainly present at pH 7.4 as pyridinium compounds substituted by a sulfonamidate function. Finally, the modulation of the intercycle linkage leads to pK_a modification in accordance with the electron-withdrawing potential of the atom or atom group of the bridge. The replacement of the oxygen atom by a sulfur atom in the trifluoromethanesulfonamide class (compounds **12i** and **13b**) did not induce a marked modification of the acidity of

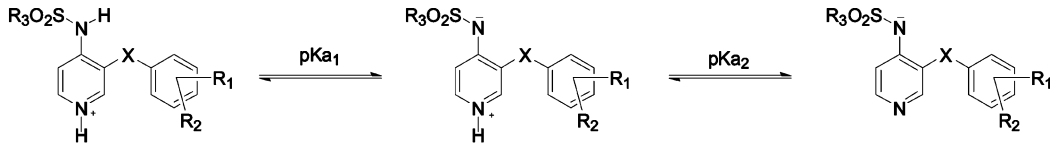

Figure 2. Attribution of pK_a values to acid−base equilibrium.

Table 3. IC_{50}(COX-1) and IC_{50}(COX-2) of Compounds **12a**−**h**, Nimesulide, and Celecoxib and the Selectivity Ratio (IC_{50}(COX-1)/IC_{50}(COX-2))

	IC_{50} (μM)		
	COX-1	COX-2	ratio
12a	0.41 ± 0.13	>100	
12b	1.03 ± 0.32	0.13 ± 0.04	7.92
12c	10.86 ± 4.08	1.99 ± 0.71	5.45
12d	1.45 ± 0.68	1.87 ± 1.56	0.77
12e	1.41 ± 0.70	7.60 ± 3.32	0.18
12f	1.81 ± 3.63	2.36 ± 1.96	0.76
12g	0.62 ± 0.04	0.12 ± 0.03	5.15
12h	>100	>100	
nimesulide	3.76 ± 1.01	0.70 ± 0.23	5.37
celecoxib	2.60 ± 0.2	0.35 ± 0.09	7.46

the analogues, while the introduction of a sulfinyl or a sulfone group generates more acidic compounds (comparison between the pK_a values obtained for compounds **12i**, **13b**, **16b**, and **17b**). In conclusion, our compounds can be classified into two groups according to their major ionic forms in solution at physiological pH: pyridinium sulfonamidate compounds bearing an alkanesulfonamide group existing as zwitterions and anionic pyridine sulfonamidate compounds bearing a trifluoromethanesulfonamide group. Because of their different ionic states at physiological pH, further evaluation and discussion were performed separately.

Pharmacological Evaluation

The synthesized compounds have been pharmacologically evaluated *in vitro* for their inhibitory potency against COX-1 and COX-2, and the selectivity ratios (IC_{50}(COX-1)/IC_{50}(COX-2)) were calculated. Selected compounds were also evaluated *in vivo* as anti-inflammatory agents in a carrageenan-induced paw oedema in rats.

The *in vitro* COX inhibitory experiments were performed using a human whole blood model. In this test, each compound was evaluated in triplicate for drug concentrations ranging from 100 to 0.01 μM. Concentration−response curves were calculated using the GraphPad Prism 3.02 software allowing the estimation of IC_{50} against both COX-1 and COX-2 enzymes. The COX-1 activity was measured as the TXB_2 production after stimulation of platelet aggregation by calcium ionophore A-23,187. The COX-2 activity was measured as the PGE_2 levels produced by leukocytes after stimulation by LPS. As previously mentioned, we have separately studied zwitterionic pyridinium and anionic pyridinic compounds.

Table 3 reports the COX-1 and COX-2 IC_{50} values (mean value of at least three independent determinations ± SEM) obtained for pyridinium compounds **12a**−**h**, nimesulide, and celecoxib. These results show that the replacement of the nitrobenzene moiety of nimesulide by a pyridine ring leads to an important loss of COX-2 inhibitory activity while the COX-1 inhibitory potency is increased. Nevertheless, substituted phenyl

Table 4. IC_{50}(COX-1) and IC_{50}(COX-2) of Compounds **12a**, **13a**, and **17a** and the Selectivity Ratio (IC_{50}(COX-1)/IC_{50}(COX-2))

	IC_{50} (μM)		
	COX-1	COX-2	ratio
12a	0.41 ± 0.13	>100	
13a	3.62 ± 0.90	1.19 ± 0.58	3.05
17a	>100	>100	

analogues of **12a** display enhanced COX-2 inhibitory activities related to the introduction of a substituent such as a halogen atom or a methoxy group in different positions. The most interesting compounds are **12b** and **12g**, which bear a chlorine atom in the 2-position (IC_{50}(COX-2): 0.13 and 0.12 μM, respectively) and appear more active toward both COX-1 and COX-2 than nimesulide and celecoxib. Moreover, in this model **12b** presents a selectivity ratio comparable to that measured with celecoxib (IC_{50} ratios: 7.92 and 7.46, respectively). Looking at the COX-1 inhibitory activity, the introduction of a substituent on the phenyl ring decreases the inhibitory potency, especially when this substituent is a halogen atom placed in the 3-position (IC_{50} against COX-1: 10.86 and >100 μM for compounds **12c** and **12h**, respectively). The more selective compounds appeared to be those characterized by a chlorine atom at the 2- or 3-position of the phenyl ring (compounds **12b**, **12c**, and **12g**). Moreover, the presence of a halogen atom in the 2-position seems to be the best compromise between the loss of activity against COX-1 and the enhancement for the COX-2 inhibition, these compounds displaying a selectivity ratio comparable to that of nimesulide. Compounds with a substituent in the 4-position were found to be COX-1 preferential inhibitors, and the introduction of a substituent in the 3-position was less favorable than in the 2-position for the obtaining of COX-2 inhibitors while double substitution at the 3- and 5-positions led to an inactive compound (**12h**).

The results obtained with compounds **12a**, **13a**, and **17a** are presented in Table 4. The replacement of the ether linkage of **12a** with a thioether linkage led to the enhancement of the COX-2 inhibitory potency (IC_{50}(COX-2): >100 μM for **12a** and 1.19 μM for **13a**) and a decrease of the COX-1 inhibitory activity. Therefore, compound **13a** was found to be a COX-2 preferential inhibitor (ratio value of 3.05). The oxidation of the sulfur atom into a sulfone linkage led to the loss of both COX-1 and COX-2 inhibitory properties (**17a**).

Another investigated modulation was the modification of the alkylsulfonamide group (Table 5). The modification of the sulfonamide moiety led to a decrease of the COX-1 inhibitory activity and, in most cases, to an enhanced COX-2 inhibition. Indeed, the replacement of the methanesulfonamide (**12a**) by an ethanesulfonamide (**12r**) or a propanesulfonamide moiety (**12t**) leads to compounds displaying decreased COX-1 inhibitory properties (IC_{50} against COX-1: 0.41, 5.34, 18.36 μM,

Table 5. IC_{50}(COX-1) and IC_{50}(COX-2) of Compounds **12a**,**d**,**r**−**u** and the Selectivity Ratio (IC_{50}(COX-1)/IC_{50}(COX-2))

	IC_{50} (μM)		
	COX-1	COX-2	ratio
12a	0.41 ± 0.13	>100	
12d	1.45 ± 0.68	1.87 ± 1.56	0.77
12r	5.34 ± 1.31	14.11 ± 5.95	0.38
12s	2.44 ± 0.70	3.28 ± 2.07	0.75
12t	18.36 ± 3.87	>100	
12u	2.30 ± 0.74	9.69 ± 13.58	0.24

Table 6. IC_{50}(COX-1) and IC_{50}(COX-2) of Compounds **12i**−**q** and Nimesulide and the Selectivity Ratio (IC_{50}(COX-1)/IC_{50}(COX-2))

	IC_{50} (μM)		
	COX-1	COX-2	ratio
12i	0.14 ± 0.01	0.62 ± 0.18	0.22
12k	0.27 ± 0.13	0.15 ± 0.06	1.74
12l	2.27 ± 0.16	>100	
12m	0.36 ± 0.01	1.53 ± 0.33	0.24
12n	0.24 ± 0.06	13.84 ± 4.61	0.02
12o	0.26 ± 0.07	0.44 ± 0.20	0.59
12p	1.37 ± 0.47	2.55 ± 1.06	0.54
12q	>100	>100	
nimesulide	3.76 ± 1.01	0.70 ± 0.23	5.37

respectively). This loss of COX-1 activity led to the conclusion that the COX-1 inhibitory activity can be correlated to the size of sulfonamide moiety. Concerning the COX-2 inhibition, the loss of the potency in the 4-chloro family (compounds **12d**, **12s**, **12u**) was also correlated to the size of the alkyl chain (IC_{50} against COX-2: 1.87, 3.28, and 9.69 μM for compounds **12d**, **12s**, and **12u**, respectively). Nevertheless, replacement of the methyl of **12a** with an ethyl radical leads to **12r**, which is a weak COX-2 inhibitor (IC_{50}(COX-2): 14.11 μM).

In the trifluoromethanesulfonamide family (Table 6) the COX-1 inhibitory activity is, in general terms, enhanced when compared to the methanesulfonamide derivatives (IC_{50} against COX-1: 0.41 and 0.14 μM for compounds **12a** and **12i**, respectively), although the introduction of a substituent on the phenyl ring leads to a slight reduction of the COX-1 inhibitory potency. Like for the methanesulfonamide class, compounds substituted in the 3-position appeared less active against both COX isozymes (IC_{50}(COX-2) > 100 μM for **12l**) and this loss of inhibitory activity was complete for compound **12q**, a 3,5-disubstituted derivative. Concerning the COX-2 inhibitory activity, the replacement of the methanesulfonamide group with a trifluoromethanesulfonamide one leads to an active COX-2 inhibitor (IC_{50}(**12a**) > 100 μM compared to IC_{50}(**12i**) = 0.62 μM). Moreover, the introduction of a chlorine atom in the 2-position significantly increased the COX-2 inhibitory potency (IC_{50}(COX-2) = 0.15 μM for **12k**).

Another variation investigated with our compounds was the linkage between the pyridine ring and the phenyl moiety. In the trifluoromethanesulfonamide family, the ether linkage of **12i** was replaced by a thioether, an amino, a sulfinyl, and a sulfone linkage. Pharmacological evaluations of these compounds are reported in Table 7. These results demonstrate that the replacement of the oxygen atom of **12i** by a sulfur atom (**13b**) leads to a decrease of the COX-1 inhibitory potency (COX-1 IC_{50}: 0.14 and 0.41 μM, respectively) and therefore to a more balanced nonselective COX

Table 7. IC_{50}(COX-1) and IC_{50}(COX-2) of Compounds **12i**, **13b**, **14b**, **15b**, **16b**, and **17b** and Nimesulide and the Selectivity Ratio (IC_{50}(COX-1)/IC_{50}(COX-2))

	IC_{50} (μM)		
	COX-1	COX-2	ratio
12i	0.14 ± 0.01	0.62 ± 0.18	0.22
13b	0.41 ± 0.27	0.53 ± 0.39	0.78
14b	0.18 ± 0.06	0.09 ± 0.03	2.03
15b	4.63 ± 1.12	47.62 ± 12.31	0.097
16b	25.61 ± 9.72	>100	
17b	>100	>100	

inhibitor (selectivity ratio of 0.22 and 0.78, respectively). In contrast, the introduction of an amino linkage enhanced the COX-2 inhibitory profile. Indeed, compound **14b** displays a greater COX-2 inhibitory profile when compared to celecoxib (IC_{50}(COX-2): 0.09 and 0.35μM, respectively), although it appears less selective against COX-2 (selectivity ratios of 2.03 and 7.46 for **14b** and celecoxib, respectively). The methylation of the amino linkage (compound **15b**) leads to a decrease of the COX inhibitory activity, especially against COX-2, and subsequently to a weak COX-1 preferential inhibitor (IC_{50}(COX-1) = 4.63 μM and IC_{50}(COX-2) = 47.62 μM). Finally, oxidation of the thioether linkage to a sulfinyl linkage leads to a weak COX-1 inhibitor (compound **16b**) while the corresponding sulfone derivative, compound **17b**, was found to be totally inactive.

These results led to the selection of compounds **12b**, **12c**, **12g**, **13a**, **14b**, which were COX-2 preferential inhibitors, for further evaluation as anti-inflammatory drugs *in vivo*. Compounds **12a** and **12i**, which are the lead compounds of the methanesulfonamide and trifluoromethanesulfonamide families, were also included in these experiments. Compounds **12d**, **12n**, and **12h**, which are a nonselective inhibitor, a COX-1 preferential inhibitor, and a nonactive COX inhibitor, respectively, were also evaluated while nimesulide was tested as a reference drug.

In these *in vivo* experiments, compounds were dissolved in DMSO and administered intraperitoneally 1 h prior to injection of 0.1 mL of a solution of λ-carrageenan in the right paw of the rat. After 3 h, the rats were euthanized and the paws were cut at the ankle. The paws were weighed, and the percentage of swelling was calculated. The results are expressed as percentage of inhibition of the swelling (mean ± SEM) compared to that of the control group (six rats per group). Table 8 reports the results obtained with our compounds and nimesulide at the doses of 3, 10, or 30 mg/kg of rat weight. In this test, nimesulide significantly inhibited the carrageenan-induced inflammation response at doses of 3, 10, and 30 mg/kg with 44% swelling inhibition at the highest concentration. Among our lead compounds, **12a** was found to be lethal at a dose of 30 mg/kg and was not studied at lower doses. In contrast, compound **12i** inhibited the inflammation at doses of 10 and 30 mg/kg. At a dose of 30 mg/kg, **12i** displayed similar anti-inflammatory properties (46% inhibition) as nimesulide and did not exhibit any observable toxicity. The COX-2 preferential inhibitor **12b** exhibited a dose-dependent anti-inflammatory profile. This compound showed an effect comparable to that observed with nimesulide at doses of 10 and 30 mg/kg with 38% and 63% swelling reduction, respectively. Compound

Table 8. *In Vivo* Evaluation of Selected Compounds[a]

compd	% inhibition of growth		
	3 mg/kg	10 mg/kg	30 mg/kg
nimesulide	23.71 ± 5.1	40.20 ± 6.18	44.32 ± 7.21
12a	ND	ND	lethal
12b	9.47 ± 22.78	37.50 ± 23.37	62.84 ± 24.29
12c	10.90 ± 20.00	21.00 ± 14.54	lethal
12d	28.72 ± 14.89	35.12 ± 11.10	lethal
12g	20.89 ± 6.24	15.82 ± 10.62	32.71 ± 11.37
12h	18.03 ± 13.11	18.03 ± 24.11	21.33 ± 14.75
12i	10.89 ± 8.91	26.03 ± 7.12	46.43 ± 16.90
12n	5.00 ± 21.60	8.33 ± 16.60	36.66 ± 21.00
13a	7.44 ± 13.58	40.74 ± 19.75	lethal
14b	22.67 ± 10.78	34.55 ± 9.37	43.95 ± 10.00

[a] The results are expressed as percentage of inhibition of the growth of the rat paw after injection of carrageenan (mean ± SEM, $n = 6$). ND: not determined.

12c, which is lethal at a dose of 30 mg/kg, displayed a weak inhibition of the inflammation at a dose of 10 mg/kg. Finally, **12g** significantly inhibited the oedema development at doses of 3 and 10 mg/kg. Results obtained at a dose of 30 mg/kg are comparable to these obtained with nimesulide. Compound **13a**, the thioether analogue of **12a**, also appeared toxic at a dose of 30 mg/kg but exhibited similar anti-inflammatory properties when compared with nimesulide at a dose of 10 mg/kg (41% inhibition). Finally, **14b** showed a similar activity compared to nimesulide and significantly inhibited the inflammatory response at the doses of 3, 10, and 30 mg/kg. This compound decreased the rat paw swelling of 34% at 10 mg/kg and 44% at 30 mg/kg. Compound **12d**, a nonselective COX inhibitor, was a weak anti-inflammatory drug at 3 mg/kg. This compound also appeared toxic at a dose of 30 mg/kg. The COX-1 preferential inhibitor **12n** and the nonactive inhibitor **12h** did not inhibit significantly the inflammation at a dose of 10 mg/kg. For **12h**, no reduction of the inflammation was observed. This result is in accordance with the effects observed *in vitro* against COX-2.

Crystallographic and Docking Studies

Besides pharmacological evaluation, crystallographic and docking studies were performed with compounds **14b** and **15b**, two structurally close compounds with very different pharmacological profiles. The crystal structures of the two compounds were resolved by X-ray diffraction and revealed, as observed for **12i**,[28] a deprotonated sulfonamide moiety and a pyridinium group (Figure 3). The conformations adopted by the two compounds are quite different. Indeed, unlike **14b**, the sulfonamide and phenyl groups of **15b** lie on the same side with respect to the pyridinium plane. This is highlighted by sulfonamide torsion angles of 84.3(2)° (C13−N14−S15−C18) and −91.1(2)° (C14−N15−S16−C19) for **14b** and **15b**, respectively. Moreover, phenyl orientation is slightly modified with torsion angles of −2.0(2)° (C8−N7−C4−C3) and 17.7(4)° (C9−N7−C4−C5). Such observations could partly justify the different behaviors of the compounds toward the COX isoforms.

Furthermore, molecular docking studies were performed on the two compounds in the human modeled isoforms. As previously described and assuming that the pK_a values of **14b** and **15b** are close to that of **12i**, the major form of the compounds at physiological pH is thought to be a pyridine sulfonamidate form. The crystal structure obtained in the solid state was used as the input conformation for the docking simulations. The active site of the two COXs is a long, narrow hydrophobic channel extending from the membrane-binding region to the protein core. The COX-2 binding site is larger (about 20%) than that of COX-1 because of the replacement of Val523 in COX-2 by a bulkier isoleucine in COX-1, which enables access to a specific lateral hydrophilic pocket, increasing the volume of COX-2.[29]

Two different binding modes were identified in the human COX-2 enzyme for the two compounds (Figure 4). Unlike **15b**, the sulfonamide group of **14b** is able to reach the hydrophilic pocket and is involved in hydrogen bonding with His90 (O···HN = 2.17Å) and Arg513 (O···HN = 1.62Å). Such interactions are essential for COX-2 inhibitory activity, as exemplified by the binding interaction of SC-558, an analogue of celecoxib cocrystallized in the COX-2 active site.[30] The lateral pocket of COX-2 would therefore be responsible for the COX-2 selectivity of **14b**. In addition, the interaction between the negative nitrogen and the amine group of **14b** ($NH\cdots N^-$ = 2.23Å) forces the phenyl ring to adopt a specific orientation at the top of the channel. This moiety is involved in a $\pi-\pi$ ($CH\cdots\pi$) interaction with Trp387. The binding mode of nimesulide, simulated by docking studies, is in agreement with results coming from the literature and is close from that of **14b** (Figure 3a).[31] As observed during the superimposition of the two binding modes, the pyridinic nitrogen of **14b** corresponds to the nitro group of nimesulide and would play the same role and particularly favorably interacts with Arg120 situated at the bottom of the channel. Because of its bulkier phenylmethylamine group, **15b** cannot take advantage of the hydrophilic side pocket in COX-2 and lies in the hydrophobic channel (Figure 4b). Although H bonding and $CH\cdots\pi$ interaction are observed between the sulfonamide moiety and Arg120 (O···NH = 1.88Å) and between the phenyl group and Trp387, the corresponding complex is less stable than the one of **14b**. The total binding energies (ΔE_{tot}), consisting of van der Waals (ΔE_{vdw}) and Columbic (ΔE_{cb}) terms and an electrostatic contribution of the solvation energy (ΔE_{solv}) (see Experimental Section), were estimated to be −26.25 and −31.99 kcal mol^{-1}, respectively. Unlike in COX-2, few differences are observed in COX-1 between **14b** and **15b** and no hypothesis concerning their COX activities could be derived from these analyses. As a result, crystallographic and docking studies show different conformations and binding modes for **14b** and **15b** and could explain the different activities of these compounds.

Conclusions

In this study, we have achieved the synthesis of pyridinic analogues of nimesulide. Obtained original compounds can be classified in two families based on their major ionic state at the physiological pH of 7.4: the zwitterionic pyridinium (alkanesulfonamides) and the anionic pyridinic (trifluoromethanesulfonamides) compounds. The results obtained from their pharmacological evaluation *in vitro* showed that pyridinium compounds are generally more selective toward COX-2

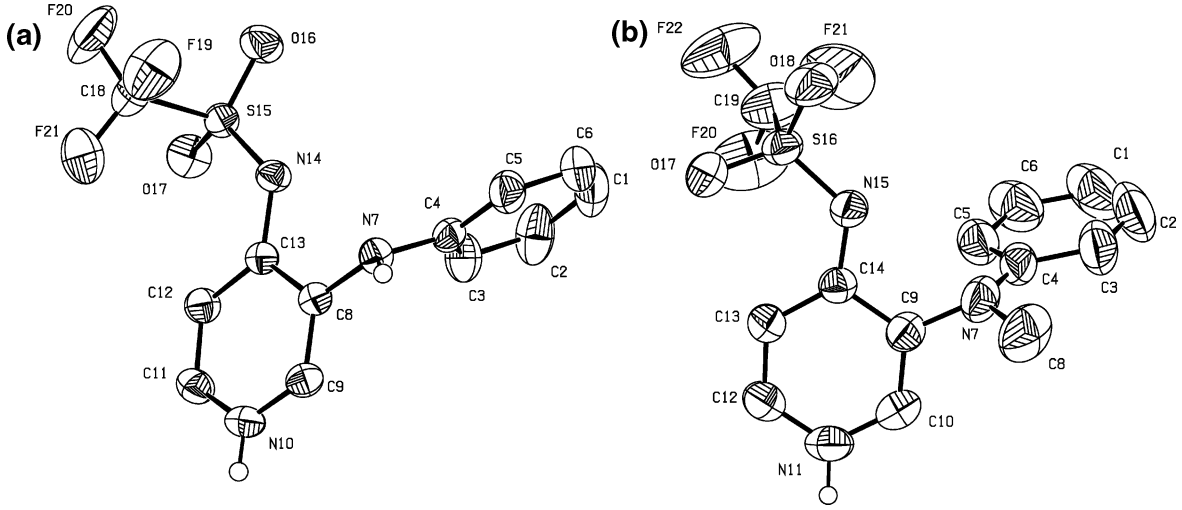

Figure 3. ORTEP illustrations of (a) **14b** and (b) **15b** (atomic displacement ellipsoids drawn at the 50% probability level). Only hydrogen atoms of nitrogen atoms are depicted.

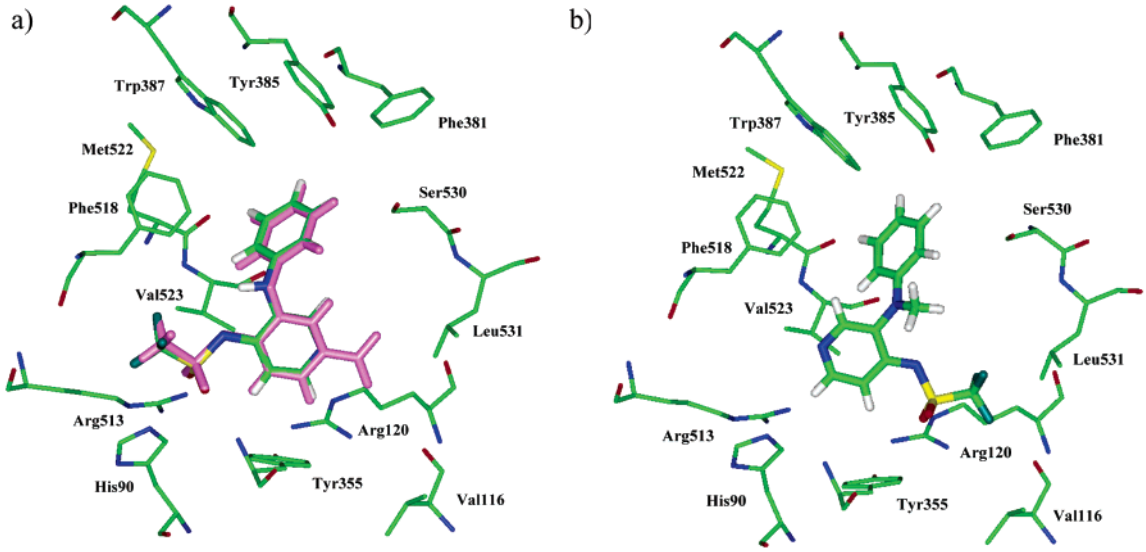

Figure 4. Potential binding mode of (a) **14b** and nimesulide (rose) and (b) **15b** in the human COX-2 active site.

when compared to their pyridinic analogues. Among these, compound **12b** displays a COX-2 selective profile similar to the profile observed with celecoxib and appears therefore to possess a better COX-2 selectivity when compared to nimesulide under our test conditions (selectivity ratio of 7.92, 7.46, and 5.37, respectively). Nevertheless, more active compounds toward the two COXs are usually found in the trifluoromethanesulfonamide group. The modulation of the linkage between the pyridinic ring and the phenyl moiety in the trifluoromethanesulfonamide class led to the development of an active and COX-2 preferential inhibitor: compound **14b**, which displays IC_{50} against COX-1 of 0.18 μM and IC_{50} against COX-2 of 0.09 μM. This compound presents a selectivity ratio of 2.02. *In vivo* experiments led to the statement that the investigated compounds possess anti-inflammatory properties. Furthermore, a positive correlation between the *in vitro* determined COX-2 inhibitory properties and *in vivo* evaluated anti-inflammatory potencies is observed with these derivatives. Our most potent COX-2 inhibitor, compound **14b** also called FJ29, shows a similar *in vivo* profile as nimesulide when tested in the rat paw oedema, while some of our compounds bearing a methanesulfonamide group appeared lethal at a dose of 30 mg/kg, although this toxicity was not observed for disubstituted compounds or compounds bearing a trifluoromethanesulfonamide group. Moreover, crystallographic and docking studies with **14b** suggest that the sulfonamide moiety and the second ring's orientation in the solid state influence the inhibitory potency on the COXs. Since no modulations of the benzene ring substitution pattern of **14b** have been performed to date and in regard to the interest of such substitution in terms of enhanced COX-2 selectivity, this compound may serve as a lead for the next generation of pyridinic sulfonamides. Finally, it is worth noting that rofecoxib has just been withdrawn worldwide because it has been demonstrated to be responsible for cardiovascular side effects related to its ability to selectively inhibit COX-2 while this side effect was not demonstrated with nonselective or preferential COX-2 inhibitors such as nimesulide. Therefore, the herein presented original derivatives, since they display preferential rather than selective COX-2 inhibition, should not be responsible for such side effects.

Experimental Section

Pharmacology. COX-1 Assay. Fresh blood was collected into heparinized tubes by venipuncture and diluted with RPMI (1:4). Aliquots of 0.25 mL of diluted blood were transferred into siliconized tubes preloaded with 1 μL of vehicle (DMSO) or test compounds at final concentrations ranging from 0.01 to 100 μmol/L. The tubes were vortexed and incubated at 37 °C under constant agitation for 15 min, and then 10 μL of calcium ionophore A-23,187 (0.2 mg/mL) was added and the aliquots were incubated for 15 min. At the end of the incubation, the serum was obtained by centrifugation (10000*g* for 10 min) and was assayed for thromboxane B_2 (TXB_2) production using an enzyme immunoassay kit (Cayman Chemical TXB_2 EIA kit, Ann Arbor, MI) according to the manufacturer's instructions.

COX-2 Assay. Fresh blood was collected in heparinized tubes by venipuncture. Aliquots of 0.5 mL of blood were transferred in heparinized tubes preloaded with either 2 μL of vehicle (DMSO) or 2 μL of test compound at final concentrations ranging from 0.01 to 100 μmol/L. The tubes were vortexed and incubated at 37°C under constant agitation for 15 min. This first treatment was followed by incubation of the blood with 10 μL of lipopolysaccharide (LPS) at a final concentration of 100 μg/mL (from *E. coli* serotype B_4) under constant agitation for 24 h at 37 °C to induce COX-2 expression. Appropriate controls (LPS replaced by 20 μL of PBS) were used as blanks. After incubation, the tubes were centrifugated at 2500*g* for 20 min in order to obtain plasma. Plasma was assayed for PGE_2 production by a specific enzyme immunoassay (Cayman Chemical PGE_2 EIA kit, Ann Arbor, MI) according to the manufacturer's instructions.

Carrageenan-Induced Rat Paw Oedema. Wistar rats (250 g) were treated with an intraperitoneal injection of the drug at the appropriate concentration (solution at a concentration of 10 mg/mL in DMSO). λ-Carragenaan (0.1 mL, 1%) was injected 1 h later into the plantar region of the right-hand paw. Three hours thereafter, the rats were euthanized by injection of nembutal (100 mg/kg) and the paws were cut at the ankle. The swelling was calculated as a percentage increase in the weight of the control paw.

Chemistry. Melting points were recorded on a Büchi 530 melting point apparatus in open capillary tubes and are uncorrected. ^{1}H NMR spectra were recorded on a Bruker DRX-400 spectrometer using DMSO-d_6 as solvent and tetramethylsilane as internal standard. For ^{1}H NMR spectra, chemical shifts are expressed in δ (ppm) downfield from tetramethylsilane. The abbreviations s = singulet, d = doublet, t = triplet, m = multiplet, and b = broad were used throughout. Elemental analyses (C, H, N, S) were determined on a Carlo-Erba EA 1108 elemental analyzer and were within ±0.4% of the theoretical values. All reactions were routinely checked by TLC on silica gel Merck 60F 254.

Compounds **3** (3-bromo-4-nitropyridine *N*-oxide) and **4a** (4-nitro-3-phenoxypyridine *N*-oxide) were synthesized following the procedure previously described.[28]

4-Nitro-3-(2-chlorophenoxy)pyridine *N*-Oxide (4b). 2-Chlorophenol (1.4 g, 10.88 mmol) was dissolved in a 2.5 M aqueous solution of NaOH (4 mL). After the mixture was stirred, the solvent was evaporated under reduced pressure. The white solid was then taken up with acetonitrile (20 mL), and the obtained suspension was heated under reflux. Then 3-bromo-4-nitropyridine *N*-oxide (2 g, 9.13 mmol) was added and the reflux was maintained for 12 h. The suspension was filtered, and the solvent was evaporated under reduced pressure. The residue was crystallized from methanol to afford 4-nitro-3-(2-chlorophenoxy)pyridine *N*-oxide as a pale-yellow solid. Yield: 45%. Mp: 123−124 °C. ^{1}H NMR (DMSO-d_6): δ 7.28−7.44 (m, 3H, H_{aro}'), 7.63−7.68 (dd, 1H, H_{aro}'), 8.09 (s, 1H, H-2), 8.25 (s, 2H, H-5 + H-6). Anal. ($C_{11}H_7ClN_2O_3$) C, H, N, S.

Compounds **4c**−**h** were similarly prepared using the appropriate substituted phenols instead of 2-chlorophenol.

4-Nitro-3-(3-chlorophenoxy)pyridine *N*-Oxide (4c). Yield: 42%. Mp: 105−106 °C. ^{1}H NMR (DMSO-d_6): δ 7.19 (dd, 1H, H-5′), 7.31 (d, 1H, H-6′), 7.8 (m, 1H, H_{aro}'), 7.43 (m, 1H, H_{aro}'), 8.21−8.29 (m, 2H, H-2 + H-6), 8.32 (d, 1H, H-5). Anal. ($C_{11}H_7ClN_2O_3$) C, H, N, S.

4-Nitro-3-(4-chlorophenoxy)pyridine *N*-Oxide (4d). Yield: 47%. Mp: 101−102 °C. ^{1}H NMR (DMSO-d_6): δ 7.0−7.4 (m, 4H, H_{aro}'), 8.0−8.1 (m, 3H, H-2 + H-5 + H-6). Anal. ($C_{11}H_7ClN_2O_4$) C, H, N, S.

4-Nitro-3-(4-bromophenoxy)pyridine *N*-Oxide (4e). Yield: 38%. Mp: 124−125 °C. ^{1}H NMR (DMSO-d_6): δ 6.8−7.0 (d, 2H, H-2′ + H-6′), 7.4−7.6 (d, 2H, H-3′ + H-5′), 8.0−8.1 (m, 3H, H-2 + H-5 + H-6). Anal. ($C_{11}H_7BrN_2O_4$) C, H, N, S.

4-Nitro-3-(4-methoxyphenoxy)pyridine *N*-Oxide (4f). Yield: 47%. Mp: 103−104 °C. ^{1}H NMR (DMSO-d_6): δ 3.76 (s, 3H, OCH_3), 7.05 (d, 2H, H-2′ + H-6′), 7.25 (d, 2H, H-3′ + H-5′), 7.76 (s, 1H, H-2), 8.1−8.2 (m, 2H, H-5 + H-6). Anal. ($C_{12}H_{10}N_2O_4$) C, H, N, S.

4-Nitro-3-(2,4-dichlorophenoxy)pyridine *N*-Oxide (4g). Yield: 53%. Mp: 142−143 °C. ^{1}H NMR (DMSO-d_6): δ 7.37−7.48 (m, 2H, H-5′ + H-6′), 7.84 (d, 1H, H-3′), 8.25 (m, 2H, H-5 + H-6), 8.30 (s, 1H, H-2). Anal. ($C_{11}H_6Cl_2N_2O_3$) C, H, N, S.

4-Nitro-3-(3,5-dichlorophenoxy)pyridine *N*-Oxide (4h). Yield: 47%. Mp: 160−161°C. ^{1}H NMR (DMSO-d_6): δ 6.73 (d, 1H, H-4′), 6.87 (d, 2H, H-2′ + H-6′), 7.29 (s, 1H, H-2), 7.96−7.98 (m, 2H, H-5 + H-6). Anal. ($C_{11}H_6Cl_2N_2O_3$) C, H, N, S.

4-Nitro-3-phenylsulfanylpyridine *N*-Oxide (5). 3-Bromo-4-nitropyridine *N*-oxide (4 g, 18.26 mmol) was dissolved in toluene (80 mL) in the presence of K_2CO_3 (2.5 g). Thiophenol (2.25 mL, 21.91 mmol) was added, and the suspension was heated under reflux for 10 h. The suspension was filtered and the toluene was evaporated under reduced pressure to give an orange solid. This solid was crystallized from ethanol to afford 4-nitro-3-phenylsulfanylpyridine *N*-oxide as a yellow solid. Yield: 55%. Mp: 147−148°C. ^{1}H NMR (DMSO-d_6): δ 7.1 (s, 1H, H-2), 7.4−7.6 (m, 5H, H_{aro}'), 8.0−8.2 (m, 2H, H-5 + H-6). Anal. ($C_{11}H_8N_2O_3S$) C, H, N, S.

4-Nitro-3-phenylaminopyridine *N*-Oxide (6). 3-Bromo-4-nitropyridine *N*-oxide (2 g, 9.13 mmol) was dissolved in freshly distilled aniline (4 mL). The solution was stirred under nitrogen at 50 °C for 5 h. Then ethyl acetate (50 mL) was added and the suspension was cooled on ice bath for 15 min. The orange solid was collected by filtration and crystallized from ethyl acetate to give the title compound. Yield: 66%. Mp: 180 °C (dec). ^{1}H NMR (DMSO-d_6): δ 7.3−7.65 (m, 5H, H_{aro}'), 7.70 (m, 2H, H-2 + H-6), 810−8.15 (d, 1H, H-5), 9.60 (s, 1H, NH). Anal. ($C_{11}H_9N_3O_3$) C, H, N, S.

***N*′-methyl-4-nitro-*N*′-phenyl-3-pyridinamine *N*-Oxide (7).** 3-Bromo-4-nitropyridine *N*-oxide (2 g, 9.13 mmol) was dissolved in freshly distilled *N*-methylaniline (10 mL). The solution was refluxed under nitrogen for 24 h. Then ethyl acetate (50 mL) was added and the resulting precipitate was collected by filtration. The solid was purified by column chromatography on silicagel using ethyl acetate as eluent to give the title compound as a red solid after evaporation. Yield: 58%. Mp: 218−219°C. ^{1}H NMR (DMSO-d_6): δ 3,34 (s, 3H, N−CH_3), 6.97−7.01 (m, 3H, H_{aro}'), 7.23−7.27 (m, 2H, H_{aro}'), 7.93 (d, 1H, H-5′), 8.05 (dd, 1H, H-6′), 8.45 (d, 1H, H-2′). Anal. ($C_{12}H_{11}N_3O_3$) C, H, N, S.

4-Amino-3-phenoxypyridine (8a). Compound **8a** was synthesized following the procedure previously described.[28]

4-Amino-3-(2-chlorophenoxy)pyridine (8b). 4-Nitro-3-(2-chlorophenoxy)pyridine *N*-oxide (0.65 g, 2.43 mmol) was dissolved in a mixture of acetic acid (15 mL) and water (5 mL). The solution was heated under reflux, and iron powder (0.67 g, 12.15 mmol) was added. The suspension was stirred for 12 h under reflux and then filtered. The filtrate was evaporated under reduced pressure. The oily residue was taken up with water, and the pH of the solution was neutralized by addition of K_2CO_3. The solution was extracted thereafter with ethyl acetate. The organic layers were dried over magnesium sulfate and evaporated under reduced pressure. 4-Amino-3-(2-chlorophenoxy)pyridine was obtained as a brown oil and was used without further purification. Yield: 66%.

The following compounds were similarly prepared.

4-Amino-3-(3-chlorophenoxy)pyridine (8c). Yield: 90%.

4-Amino-3-(4-chlorophenoxy)pyridine (8d). Yield: 89%.

4-Amino-3-(4-bromophenoxy)pyridine (8e). Yield: 82%. ^{1}H NMR (DMSO-d_6): δ 5.87 (bs exchangeable, 2H, NH_2), 6.59−6.84 (m, 3H, H-5 + H-2′ + H-6′), 7.36 (d, 2H, H-3′ + H5′), 7.82−7.91 (m, 2H, H-2 + H-6).

4-Amino-3-(4-methoxyphenoxy)pyridine (8f). Yield: 75%.

4-Amino-3-(2,4-dichlorophenoxy)pyridine (8g). Yield: 41%.

4-Amino-3-(3,5-dichlorophenoxy)pyridine (8h). Yield: 72%.

4-Amino-3-phenylsulfanylpyridine (9). Yield: 77%.

4-Amino-3-phenylaminopyridine (10). Yield: 52%.

4-Amino-*N*′-methyl-*N*′-phenyl-3-pyridinamine (11). Yield: 60%.

***N*-(3-Phenoxy-4-pyridinyl)methanesulfonamide (12a) and *N*-(3-Phenoxy-4-pyridinyl)trifluoromethanesulfonamide (12i). 12a** and **12i** were synthesized following the procedure previously described.[28]

***N*-(3-(2-Chlorophenoxy)-4-pyridinyl)methanesulfonamide (12b).** Anhydrous potassium carbonate (8.29 g, 60 mmol) was added to 4-amino-3-(2-chlorophenoxy)pyridine (2.20 g, 10 mmol) dissolved in dry acetonitrile (112 mL). The suspension was stirred for 5 min, and methanesulfonyl chloride (3.11 mL, 60 mmol) was added. The suspension was stirred for 6 h and filtered, and the solvent was evaporated under reduced pressure. The residue was taken up with a 10% aqueous solution of NaOH, and the resulting solution was neutralized with 1 N HCl to precipitate the title compound as a white solid. Yield: 76%. Mp: 208−209 °C. ^{1}H NMR (DMSO-d_6): δ 2.50 (s, 3H, CH_3), 6.86 (d, 1H, H-6′), 7.12 (t, 1H, H-5′), 7.28 (m, 1H, H-4′), 7.41 (d, 1H, H-3′), 7.54 (dd, 1H, H-5), 8.01−8.07 (m, 2H, H-2 + H6). Anal. ($C_{12}H_{11}ClN_2O_3S$) C, H, N, S.

The following compounds were similarly were prepared.

***N*-[3-(3-Chlorophenoxy)-4-pyridinyl]methanesulfonamide (12c).** Yield: 52%. Mp: 172−173 °C. ^{1}H NMR (DMSO-d_6): δ 2.79 (s, 3H, CH_3), 6.88 (dd, 1H, H-4′), 6.98 (s, 1H, H-2′), 7.13 (d, 1H, H-6′), 7.36 (t, 1H, H-5′), 7.44 (d, 1H, H-5), 8.06 (d, 1H, H-6), 8.18 (s, 1H, H-2). Anal. ($C_{12}H_{11}ClN_2O_3S$) C, H, N, S.

***N*-[3-(4-Chlorophenoxy)-4-pyridinyl]methanesulfonamide (12d).** Yield: 64%. Mp: 213-214 °C. ^{1}H NMR (DMSO-d_6): δ 2.75 (s, 3H, CH_3), 6.90−6.95 (m, 2H, H-2′ + H-6′), 7.20−7.40 (m, 3H, H-5 + H-3′ + H-5′), 7.90−8.10 (m, 2H, H-2 + H-6). Anal. ($C_{12}H_{11}ClN_2O_3S$) C H, N, S.

***N*-[3-(4-Bromophenoxy)-4-pyridinyl]methanesulfonamide (12e).** Yield: 73%. Mp: 224−225 °C. ^{1}H NMR (DMSO-d_6): δ 2.73 (s, 3H, CH_3), 6.90−6.95 (d, 2H, H-2′ + H-6′), 7.25−7.50 (m, 3H, H-5 + H-3′ + H-5′), 8.00−8.10 (m, 2H, H-2 + H-6). Anal. ($C_{12}H_{11}BrN_2O_3S$) C, H, N, S.

***N*-[3-(4-Methoxyphenoxy)-4-pyridinyl]methanesulfonamide (12f).** Yield: 68%. Mp: 188−189 °C. ^{1}H NMR (DMSO-d_6): δ 2.91 (s, 3H, CH_3), 3.72 (s, 3H, OCH_3), 6.90−7.0 (m, 4H, H_{aro}′), 7.41 (d, 1H, H-5), 7.88 (s, 1H, H-2), 8.03 (d, 1H, H-6), 11.5 (bs, 1H, N−H). Anal. ($C_{13}H_{14}N_2O_4S$) C, H, N, S.

***N*-[3-(2,4-Dichlorophenoxy)-4-pyridinyl]methanesulfonamide (12g).** Yield: 57%. Mp: 205−206 °C. ^{1}H NMR (DMSO-d_6): δ 2.75 (s, 3H, CH_3), 6.75 (d, 1H, H-6′), 7.15−7.60 (m, 3H, H-5 + H-3′ + H-5′), 7.90−8.10 (m, 2H, H-2 + H-6). Anal. ($C_{12}H_{10}Cl_2N_2O_3S$) C, H, N, S.

***N*-[3-(3,5-Dichlorophenoxy)-4-pyridinyl]methanesulfonamide (12h).** Yield: 78%. Mp: 126−127 °C. ^{1}H NMR (DMSO-d_6): δ 2.60 (s, 3H, CH_3), 6.90 (s, 2H, H-2′ + H-6′), 7.2 (s, 1H, H-4′), 7.35 (d, 1H, H-5), 8.00 (d, 1H, H-6), 8.20 (s, 1H, H-2). Anal. ($C_{12}H_{10}Cl_2N_2O_3S$) C, H, N, S.

***N*-[3-(2-Chlorophenoxy)-4-pyridinyl]trifluoromethanesulfonamide (12j).** Yield: 51%. Mp: 204−205 °C. ^{1}H NMR (DMSO-d_6): δ 6.80 (dd, 1H, H′-6), 7.09−7.14 (m, 1H, H′-5), 7.22−7.27 (m, 1H, H′-4), 7.54 (dd, 1H, H′-3), 7.75 (d, 1H, H-5), 8.30 (d, 1H, H-6), 8.45 (s, 1H, H-2). Anal. ($C_{12}H_8ClF_3N_2O_3S$) C, H, N, S.

***N*-[3-(3-Chlorophenoxy)-4-pyridinyl]trifluoromethanesulfonamide (12k).** Yield: 59%. Mp: 198−199 °C. ^{1}H NMR (DMSO-d_6): δ 6.87−7.95 (m, 2H, H-2′ + H-6′), 7.13 (d, 1H, H-4′), 7.30 (t, 1H, H-5′), 7.75 (d, 1H, H-5), 8.10 (d, 1H, H-6), 8.55 (s, 1H, H-2), 13.90 (bs, 1H, NH). Anal. ($C_{12}H_8ClF_3N_2O_3S$) C, H, N, S.

***N*-[3-(4-Chlorophenoxy)-4-pyridinyl]trifluoromethanesulfonamide (12l).** Yield: 63%. Mp: 222−223 °C. ^{1}H NMR (DMSO-d_6): δ 6.92 (d, 2H, H′-2 + H′6), 7.35 (d, 2H, H′-3 + H′-5), 7.75 (d, 1H, H-5), 8.27 (d, 1H, H-6), 8.48 (s, 1H, H-2). Anal. ($C_{12}H_8ClF_3N_2O_3S$) C, H, N, S.

***N*-[3-(4-Bromophenoxy)-4-pyridinyl]trifluoromethanesulfonamide (12m).** Yield: 71%. Mp: 245−246 °C. ^{1}H NMR (DMSO-d_6): δ 6.87 (d, 2H, H-2′ + H-6′), 7.48 (d, 2H, H-3′ + H-5′), 7.75 (d, 1H, H-5), 8.26 (d, 1H, H-6), 8.46 (s, 1H, H-2). Anal. ($C_{12}H_8BrF_3N_2O_3S$) C, H, N, S.

***N*-[3-(4-Methoxyphenoxy)-4-pyridinyl]trifluoromethanesulfonamide (12n).** Yield: 56%. Mp: 191−192 °C. ^{1}H NMR (DMSO-d_6): δ 3.72 (s, 3H, OCH_3), 6.91−6.96 (m, 4H, H′$_{aro}$), 7.72 (d, 1H, H-5), 8.17−8.23 (m, 2H, H-2 + H-6). Anal. ($C_{13}H_{11}F_3N_2O_4S$) C, H, N, S.

***N*-[3-(2,4-Dichlorophenoxy)-4-pyridinyl]trifluoromethanesulfonamide (12o).** Yield: 71%. Mp: 171−172 °C. ^{1}H NMR (DMSO-d_6): δ 6.85 (d, 1H, H-6′), 7.33 (d, 1H, H-5′), 7.70 (m, 2H, H-5 + H-3′), 8.28 (d, 1H, H-6), 8.55 (s, 1H, H-2), 14.05 (bs, 1H, NH^+). Anal. ($C_{12}H_7Cl_2F_3N_2O_3S$) C, H, N, S.

***N*-[3-(3,5-Dichlorophenoxy)-4-pyridinyl]trifluoromethanesulfonamide (12p).** Yield: 67%. Mp: 219−220 °C. ^{1}H NMR (DMSO-d_6): δ 7.01 (m, 2H, H′-2 + H′-6), 7.29 (m, 1H, H′-4), 7.77 (d, 1H, H-5), 8.31 (d, 1H, H-6), 8.57 (s, 1H, H-2). Anal. ($C_{12}H_7Cl_2F_3N_2O_3S$) C, H, N, S.

***N*-(3-Phenoxy-4-pyridinyl)ethanesulfonamide (12q).** Yield: 63%. Mp: 128−129 °C. ^{1}H NMR (DMSO-d_6): δ 0.95 (t, 3H, CH_3), 2.85 (bm, 2H, CH_2), 6.91 (d, 2H, H-2′ + H-6′), 7.06 (t, 1H, H-4′), 7.33 (t, 2H, H-3′ + H-5′), 7.42 (d, 1H, H-5), 8.02 (bs, 1H, H-6), 8.08 (s, 1H, H-2). Anal. ($C_{13}H_{14}N_2O_3S$) C, H, N, S.

***N*-[3-(4-Chlorophenoxy)-4-pyridinyl]ethanesulfonamide (12r).** Yield: 79%. Mp: 133−134 °C. ^{1}H NMR (DMSO-d_6): δ 0.95 (t, 3H, CH_3), 2.80 (bm, 2H, CH_2), 6.92 (d, 2H, H-2′ + H-6′), 7.35−7.43 (m, 3H, H-5 + H-3′ + H-5′), 8.0 (m, 1H, H-6), 8.16 (s, 1H, H-2). Anal. ($C_{13}H_{13}ClN_2O_3S$) C, H, N, S.

***N*-(3-Phenoxy-4-pyridinyl)propanesulfonamide (12s).** Yield: 61%. Mp: 191−192 °C. ^{1}H NMR (DMSO-d_6): δ 0.79 (t, 3H, CH_3), 1.45 (m, 2H, CH_2), 2.80 (bm, 2H, CH_2), 6.91 (d, 2H, H-2′ + H-6′), 7.06 (t, 1H, H-4′), 7.29−7.35 (t, 2H, H-3′ + H-5′), 7.42 (d, 1H, H−H-5), 8.02 (bs, 1H, H-6), 8.11 (s, 1H, H-2). Anal. ($C_{14}H_{16}N_2O_3S$) C, H, N, S.

***N*-[3-(4-Chlorophenoxy)-4-pyridinyl]propanesulfonamide (12t).** Yield: 47%. Mp: 121−122 °C. ^{1}H NMR (DMSO-d_6): δ 0.80 (t, 3H, CH_3), 1.35 (m, 2H, CH_2), 2.75 (bm, 2H, CH_2), 6.92 (d, 2H, H-2′ + H-6′), 7.33−7.42 (m, 3H, H-5 + H-3′ + H-5′), 8.01 (m, 1H, H-6), 8.16 (s, 1H, H-2). Anal. ($C_{14}H_{15}ClN_2O_3S$) C, H, N, S.

***N*-(3-Phenylsulfanyl-4-pyridinyl)methanesulfonamide (13a).** Yield: 53%. Mp: 180−181 °C. ^{1}H NMR (DMSO-d_6): δ 2.82 (s, 3H, CH_3), 7.21 (d, 1H, H-5), 7.32 (s, 1H, H-2), 7.49 (m, 5H, H′$_{aro}$), 7.92 (d, 1H, H-6), 13.60 (bs, 1H, H^+). Anal. ($C_{12}H_{12}N_2O_3S_2$) C, H, N, S.

***N*-(3-Phenylsulfanyl-4-pyridinyl)trifluoromethanesulfonamide (13b).** Yield: 59%. Mp: 188−189 °C. ^{1}H NMR (DMSO-d_6): δ 7.52−7.59 (m, 3H, H-2′ + H-4′ + H-6′), 7.70 (t, 2H, H-3′ + H-5′), 7.93 (d, 1H, H-5), 8.35 (d, 1H, H-6), 9.03 (s, 1H, H-2). Anal. ($C_{12}H_9F_3N_2O_3S$) C, H, N, S.

***N*-(3-Phenylamino-4-pyridinyl)trifluoromethanesulfonamide (14b).** Yield: 42%. Mp: 188−189 °C. ^{1}H NMR (DMSO-d_6): δ 7.05 (t, 1H, H-4′), 7.28−7.42 (m, 5H, H′$_{aro}$ + NH), 7.62 (d, 1H, H-5), 7.97 (d, 1H, H-6), 8.05 (s, 1H, H-2), 13.60 (bs, 1H, N−H^+). Anal. ($C_{12}H_{10}F_3N_3O_2S$) C, H, N, S.

***N*-[3-(*N*′-Methyl-*N*′-phenylamino)-4-pyridinyl]trifluoromethanesulfonamide (15b).** Yield: 59%. Mp: 218−219 °C. ^{1}H NMR (DMSO-d_6): δ 3.12 (s, 3H, N−CH_3), 6.58 (d, 2H, H-2′ + H-6′), 6.72 (t, 1H, H-4′), 7.11−7.18 (m, 2H, H-3′ + H-5′), 7.76 (d, 1H, H-5), 8.25 (d, 1H, H-6), 8.35 (s, 1H, H-2). Anal. ($C_{13}H_{12}F_3N_2O_2S$) C, H, N, S.

***N*-(3-Phenylsulfinyl-4-pyridinyl)trifluoromethanesulfonamide (16b).** *N*-(3-Phenylsulfanyl-4-pyridinyl)trifluoromethanesulfonamide (0.1 g, 0.29 mmol) was dissolved in dichloromethane (10 mL). Then *m*-chloroperbenzoic acid (0.056 g, 0.32 mmol) was added and the solution was stirred for 2 h.

The title compound was collected by filtration as a white solid and dried under vacuum. Yield: 87%. Mp: 273−274 °C. ^{1}H NMR (DMSO-d_6): δ 7.49−7.55 (m, 4H, H_{aro}'), 7.76−7.79 (m, 2H, H-5 + H_{aro}'), 8.38 (dd, 1H, H-6), 8.67 (d, 1H, H-2). Anal. ($C_{12}H_9F_3N_2O_3S_2$) C, H, N, S.

***N*-(3-Phenylsulfonyl-4-pyridinyl)methanesulfonamide (17a).** *N*-(3-Phenylsulfanyl-4-pyridinyl)methanesulfonamide (0.25 g, 0.89 mmol) was dissolved in glacial acetic acid (10 mL). Then a 30% hydrogen peroxide solution (78 μL) was added and the solution was stirred for 24 h at room temperature. The solvent was evaporated under reduced pressure and the oily residue was crystallized from ethyl acetate to afford *N*-(3-phenylsulfonyl-4-pyridinyl)methanesulfonamide as a white solid. Yield: 73%. Mp: 221−222 °C. ^{1}H NMR (DMSO-d_6): δ 2.74 (s, 3H, CH_3), 7.16 (d, 1H, H-5), 7.48−7.56 (m, 3H, H_{aro}'), 7.80−7.85 (m, 2H, H_{aro}'), 8.03 (d, 1H, H-6), 8.32 (s, 1H, H-2). Anal. ($C_{12}H_{12}N_2O_4S_2$) C, H, N, S.

***N*-(3-Phenylsulfonyl-4-pyridinyl)trifluoromethanesulfonamide (17b).** *N*-(3-Phenylsulfanyl-4-pyridinyl)trifluoromethanesulfonamide (0.3 g, 0.89 mmol) was dissolved in glacial acetic acid (10 mL). The solution was heated under reflux, and a 30% hydrogen peroxide solution (78 μL) was added. The solution was stirred for 4 h under reflux. The solution was then evaporated under reduced pressure. The residue was crystallized from water to afford the title compound as a white solid. Yield: 79%. Mp: 217−218 °C. ^{1}H NMR (DMSO-d_6): δ 7.49−7.5 (m, 5H, H'_{aro}), 7.95 (d, 1H, H-5), 8.35 (d, 1H, H-6), 9.05 (s, 1H, H-2). Anal. ($C_{12}H_9F_3N_2O_4S_2$) C, H, N, S.

pK_a Determination. The determination and the calculation of the pK_a values were achieved according to a previously described procedure.[28]

X-ray Studies. Crystals of compounds **14b** and **15b** for X-ray analysis were prepared by growth under slow evaporation at room temperature of MeOH solution of each compound. Diffraction data were collected on an Enraf-Nonius CaD-4 diffractometer by use of monochromatized Cu Kα radiation (λ=1.541 78 Å). An analytical absorption correction was applied. The structure of each compound was solved and refined on F^2 with the SIR97[32] and SHELXL97[33] programs.

Docking Studies. Because human COX-1 and -2 structures are not yet available in the PDB databank, they were first modeled by homology from the ovine COX-1 cocrystallized with flurbiprofen (1CQE) and from the murine COX-2 complexed with SC558 (6COX), respectively. This was performed using the package HOMOLOGY in Insight II.[34] Then three docking algorithms were first used: GOLD, RESEARCH, and AUTODOCK.[35−37] GOLD is a genetic algorithm used to dock flexible ligands into protein binding sites. Conformation of some amino acids (Ser, Thr, and Lys) are optimized during the run. Popsiz = 100; maxops = 100 000; niche_size = 2.

RESEARCH performs exploration of one region of the protein (rigid) by one ligand (flexible). The hypothesis generation is based on a Monte Carlo algorithm, randomly generating conformations. Cutoff = 15Å; E_{cut} = −10 kcal/mol; n_{trials} = 10000.

AUTODOCK uses a hybrid method called Lamarckian genetic algorithm (genetic algorithm coupled with a local search) to predict the interaction of ligands with macromolecular targets. Runs = 200; population size = 50; number of generations = 27 000.

The solutions shared by the three programs were then optimized with DISCOVER3 from the Insight II software[38] in order to relax the amino acids of the active site. The ESFF force field was used, and two minimization steps were applied: the steepest descent and the conjugated gradient algorithms with convergence criteria of 0.01 and 0.001 kcal/mol, respectively. The backbone moves following force constants and side chains move freely. A dielectric constant of 1*r* was used. A binding energy with van der Waals (ΔE_{vdw}) and Columbic (ΔE_{cb}) terms are calculated by DISCOVER3.

DELPHI provides numerical solutions to the Poisson−Boltzmann equation for molecules of arbitrary shape and charge distribution. It allows calculation of the electrostatic contribution to the solvation energy of a molecule (ΔE_{solv}).[39]

Acknowledgment. This study was supported by grants from the "Communauté Française de Belgique" and the "Leon Frédéricq Foundation".

Supporting Information Available: Elemental analysis of the compounds and crystallographic data for compounds **14b** and **15b**. This material is available free of charge via the Internet at http://pubs.acs.org.

References

(1) Yucel, T.; Ahola, H.; Carlsted, J.; Modeer, T. Involvement of tyrosine kinases on cyclooxygenase expression and prostaglandin E_2 production in human gingival fibroblasts stimulated with interleukin-1beta and epidermal growth factor. *Biochem. Biophys. Res. Commun.* **1999**, *257* (2), 528−532.
(2) Smith, W.; De Witt, D.; Garavito, R. Structural, cellular, and molecular biology. *Annu. Rev. Biochem.* **2000**, *69*, 145−182.
(3) Crofford, L.; Wilder, R.; Ristimaki, A.; Sano, H.; Remmers, E.; Epps, H.; Hla, T. Cyclooxygenase-1 and -2 expression in rheumatoid synovial tissues. Effects of interleukin-1 beta, phorbol ester, and corticosteroids. *J. Clin. Invest.* **1994**, *93* (3), 1095−1101.
(4) Mifflin, R.; Saada, J.; Di Mari, J.; Adegboyega, P.; Valentich, J.; Powell, D. Regulation of COX-2 expression in human intestinal myofibroblasts: mechanisms of IL-1-mediated induction. *Am. J. Physiol.: Cell Physiol.* **2002,** *282* (4), C824−834.
(5) Cao, C.; Matsumura, K.; Shirakawa, N.; Maeda, M.; Jikihara, I.; Watanabe, Y. Pyrogenic cytokines injected into the rat cerebral ventricle induce cyclooxygenase-2 in brain endothelial cells and also upregulate their receptors. *Eur. J. Neurosci.* **2001**, *13* (9), 1781−1790.
(6) Samad, T.; Moore, K.; Sapirstein, A.; Billet, S.; Allchorne, A.; Poole, S.; Bonventre, J.; Woolf, C. Interleukin-1beta-mediated induction of COX-2 in the CNS contributes to inflammatory pain hypersensitivity. *Nature* **2001**, *410*, 471−475.
(7) lopez, L.; Alonso, A.; Bayon, Y.; Nieto, M.; Orduna, A.; Sanchez, M. Brucella lipopolysaccharides induce cyclooxygenase-2 expression in monocytic cells. *Biochem. Biophys. Res. Commun.* **2001**, *289* (2), 372−375.
(8) Devaux, Y.; Seguin, C.; Grosjean, S.; de Talance, N.; Camaeti, V.; Burlet, A.; Zannad, F.; Meistelman, C.; Mertes, P.; Longrois, D. Lipopolysaccharide-induced increase of prostaglandin E(2) is mediated by inducible nitric oxide synthase activation of the constitutive cyclooxygenase and induction of membrane-associated prostaglandin E synthase. *J. Immunol.* **2001**, *167* (7), 3962−3971.
(9) Futaki, N.; Takahashi, S.; Kitagawa, T.; Yamakawa, Y.; Tanaka, M.; Higuchi, S. Selective inhibition of cyclooxygenase-2 by NS-398 in endotoxin shock rats *in vivo*. *Inflammation Res.* **1997**, *46* (12), 496−502.
(10) Wallace, J. Pathogenesis of NSAID-induced gastroduodenal mucosal injury. *Best Pract. Res. Clin. Gastroenterol.* **2001**, *15* (5), 691−703.
(11) Cryer, B. Mucosal defense and repair. Role of prostaglandins in the stomach and duodenum. *Gastroenterol. Clin. North Am.* **2001**, *30* (4), 877−894.
(12) Coffey, R.; Hawkey, C.; Damstrup, L.; Graves-Deal, R.; Daniel, V.; Dempsey, P.; Chinery, R.; Kirkland, S.; DuBois, R.; Jetton, T.; Morrow, J. Epidermal growth factor receptor activation induces nuclear targeting of cyclooxygenase-2, basolateral release of prostaglandins, and mitogenesis in polarizing colon cancer cells. *Proc. Natl. Acad. Sci. U.S.A.* **1997**, *94* (2), 657−662.
(13) Mitchell, J.; Evans, T. Cyclooxygenase-2 as a therapeutic target. *Inflammation Res.* **1998**, *47* (S2), S88−S92.
(14) Cao, Y.; Prescott, S. Many actions of cyclooxygenase-2 in cellular dynamics and in cancer. *J. Cell. Physiol.* **2002**, *190* (3), 279−286.
(15) Chan, G.; Boyle, J.; Yang, E.; Zhang, F.; Sacks, P.; Shah, J.; Edelstein, D.; Soslow, R.; Koki, A.; Woerner, B.; Masferrer, J.; Dannenberg, A. Cyclooxygenase-2 expression is up-regulated in squamous cell carcinoma of the head and neck. *Cancer Res.* **1999**, *59* (5), 991−994.
(16) Half, E.; Tang, X.; Gwyn, K.; Sahin, A.; Wathen, K.; Sinicrope, F. Cyclooxygenase-2 expression in human breast cancers and adjacent ductal carcinoma in situ. *Cancer Res.* **2002**, *62* (6), 1676−1681.
(17) Brodie, A.; Lu, Q.; Long, B.; Fulton, A.; Chen, T.; Macpherson, N.; DeJong, P.; Blankenstein, M.; Nortier, J.; Slee, P.; van de Ven, J.; van Grop, J.; Elbers, J.; Schipper, M.; Blijham, G.;

Thijssen, J. Aromatase and COX-2 expression in human breast cancers. *J. Steroid Biochem. Mol. Biol.* **2001**, *79*, 41−47.
(18) Yoshimatsu, K.; Altorki, N.; Golijanin, D.; Zhang, F.; Jakobsson, P.; Dannenberg, A.; Subbaramaiah, K. Inducible prostaglandin E synthase is overexpressed in non-small cell lung cancer. *Clin. Cancer Res.* **2001**, *7* (9), 2669−2674.
(19) Dannenberg, A.; Altorki, N.; Boyle, J.; Lin, D.; Subbaramaiah, K. Inhibition of cyclooxygenase-2: an approach to preventing cancer of the upper aerodigestive tract. *Ann. N.Y. Acad. Sci.* **2001**, *952*, 109−115.
(20) Taketo, M. COX-2 and colon cancer. *Inflammation Res.* **1998**, *47*, S112−S116.
(21) Maekawa, M.; Sugano, K.; Sano, H.; Miyazaki, S.; Ushiama, M.; Fujita, S.; Gotoda, T.; Yokota, T.; Ohkura, H.; Kakizoe, T.; Sekiya, T. Increased expression of cyclooxygenase-2 to -1 in human colorectal cancers and adenomas, but not in hyperplastic polyps. *Jpn. J. Clin. Oncol.* **1998**, *28* (7), 421−426.
(22) Niijima, M.; Yamaguchi, T.; Ishihara, T.; Hara, T.; Kato, K.; Kondo, F.; Saisho, H. Immunohistochemical analysis and in situ hybridization of cyclooxygenase-2 expression in intraductal papillary-mucinous tumors of the pancreas. *Cancer* **2002**, *94* (5), 1565−1573.
(23) Lee, L.; Pan, C.; Cheng, C.; Chi, C.; Liu, T. Expression of cyclooxygenase-2 in prostate adenocarcinoma and benign prostatic hyperplasia. *Anticancer Res.* **2001**, *21* (2B), 1291−1294.
(24) Masferrer, J. Approach to angiogenesis inhibition based on cyclooxygenase-2. *Cancer J.* **2001**, *7* (S3), S144−S150.
(25) Sinicrope, F.; Half, E.; Morris, J.; Lynch, P.; Morrow, J.; Levin, B.; Hawk, E.; Cohen, D.; Ayers, G.; Stephens, L. Familial Adenomatous Polyposis Study Group. Cell proliferation and apoptotic indices predict adenoma regression in a placebo-controlled trial of celecoxib in familial adenomatous polyposis patients. *Cancer Epidemiol., Biomarkers Prev.* **2004**, *13* (6), 920−927.
(26) Supuran, C.; Casini, A,; Mastrolorenzo, A.; Scozzafava, A. COX-2 selective inhibitors, carbonic anhydrase inhibition and anticancer properties of sulfonamides belonging to this class of pharmacological agents. *Mini-Rev. Med. Chem.* **2004**, *4*, 625−632.
(27) Danhardt, G.; Kiefer, W. Cyclooxygenase inhibitors current status and future prospects. *Eur. J. Med. Chem.* **2001**, *36*, 109−126.
(28) Julemont, F.; de Leval, X.; Michaux, C.; Damas, J.; Charlier, C.; Durant, F.; Pirotte, B.; Dogne, J. Spectral and Crystallographic Study of Pyridinic Analogues of Nimesulide: Determination of the Active Form of Methanesulfonamides as COX-2 Selective Inhibitors. *J. Med. Chem.* **2002**, *45*, 5182−5185.
(29) Michaux, C.; Charlier, C. Structural approach for COX-2 inhibition. *Mini-Rev. Med. Chem.* **2004**, *4*, 603−615.
(30) Kurumbail, R. G.; Stevens, A. M.; Gierse, J. K.; McDonald, J. J.; Stegeman, R. A.; Pak, J. Y.; Gildehaus, D.; Miyashiro, J. M.; Penning, T. D.; Seibert, K.; Isakson, P. C.; Stallings, W. C. Structural basis for selective inhibition of cyclooxygenase-2 by anti-inflammatory agents. *Nature* **1996**, *384*, 644−648.
(31) Garcia-Nieto, R.; Pérez, C.; Gago, F. Automated docking and molecular dynamics simulations of nimesulide in the cyclooxygenase active site of human prostaglandin-endoperoxide synthase-2 (COX-2). *J. Comput.-Aided Mol. Des.* **2000**, *14*, 147−160.
(32) Altomare, A.; Burla, M. C.; Camalli, M.; Cascarano, G.; Giacovazzo, C.; Guagliardi, A.; Moliterni, A. G. G.; Polidori, G.; Spagna, R. SIR97: a new tool for crystal structure determination and refinement. *J. Appl. Crystallogr.* **1999**, *32*, 115−119.
(33) Sheldrick, G. M. *SHELXL97: Program for the Refinement of Crystal Structures*; Institüt für Anorganische Chemie der Universität Göttingen: Göttingen, Germany, 1997.
(34) Biosym/MSI. *Insight II 97.0: HOMOLOGY*; Molecular Simulations Inc.: San Diego, CA, 1997.
(35) Jones, G.; Willett, P.; Glen, R. C.; Leach, A. R.; Taylor, R. *GOLD*, version 1.2, Astex Technology: Cambridge, U.K., 2001.
(36) Hart, T. N.; Ness, S. R. *Dockvision*, version 1.0.3, Alberta, CA, 1998.
(37) Morris, G. M.; Goodsell, D. S.; Halliday, R. S.; Huey, R.; Hart, W. E.; Belew, R. K.; Olson, A. J. Automated docking using a Lamarckian genetic algorithm and an empirical binding free energy function. *J. Comput. Chem.* **1998**, *19*, 1639−1662.
(38) *Discover3*, version 2.98, Accelrys Inc.: San Diego, CA, 1998.
(39) Honig, B.; Sharp, K. A.; Yang, A.-S. Macroscopic models of aqueous solutions: biological and chemical applications. *J. Phys. Chem.* **1993**, *97*, 1101−1109.

JM049480L